Squeezed singly resonant second-harmonic generation in periodically poled lithium niobate

M. J. Lawrence, R. L. Byer, and M. M. Fejer

Ginzton Laboratory, Stanford University, Stanford, California 94560

W. Bowen, P. K. Lam, and H.-A. Bachor

Department of Physics, Australian National University, Canberra, ACT, Australia

Received June 21, 2001; revised manuscript received January 9, 2002

We determine the theoretical singly resonant second-harmonic generation squeezing performance of several cavity designs and nonlinear materials. We show that, for the doubling of the 1064-nm output of Nd:YAG lasers, monolithic cavities made from periodically poled $LiNbO_3$ (PPLN) will produce the largest amount of squeezing. We also present experimental results for a free-space cavity with a PPLN sample that yielded slightly less than 0.6 dB of measured squeezing. The cavity performance as a function of input power agrees with our theoretical predictions and shows the superior performance of periodically poled materials for the production of bright squeezed light. © 2002 Optical Society of America

OCIS codes: 190.4410, 190.2620, 160.4330, 270.6570.

1. INTRODUCTION

Since 1988,[1] second-harmonic generation (SHG) has been proved an effective means of generating bright, squeezed light. In particular, a singly resonant frequency doubler, in which only the fundamental wavelength resonates within the cavity that contains the nonlinear medium, offers several technical advantages.[2] Ultimately the amount of squeezing that is possible is limited by noise in the fundamental beam, the losses encountered during and after the nonlinear process, and the strength of the nonlinear interaction.

Noise in the fundamental beam is coupled to the output at the second harmonic, reducing the amount of squeezing.[3] Fortunately, one can reduce the noise on the pump beam to the shot-noise limit in the megahertz range by passing it through a ring mode cleaner of suitable finesse.[4,5]

Losses encountered during and after the nonlinear process decrease the efficiency of the nonlinear interaction and allow vacuum (nonsqueezed) fields to enter the system. Apart from the inevitable losses from the nonlinear material itself, material interfaces are the greatest source of loss within the cavity. Monolithic resonators, for which the nonlinear material defines the cavity, can reduce the overall loss by reducing the number of interfaces in the optical path. This advantage has been recognized and exploited for efficient SHG and optical parametric oscillator experiments,[6,7] as well as for several squeezing experiments.[3,8–10]

Strong nonlinear interaction requires phase matching between the interacting fields. When they are phase matched these fields propagate in phase through the nonlinear medium, resulting in the strongest possible coupling. Typically, crystal birefringence is used to offset dispersion. However, this method requires that the fields be orthogonally polarized. The strength of the resulting nonlinear coupling is determined by a small off-diagonal element of the $\chi^{(2)}$ tensor. In quasi-phase-matched materials, periodic reversals of the sign of the nonlinear coefficient obtained by periodic reversals of the ferroelectric domains are used to counteract dispersion.[11] This procedure permits the use of interacting fields with the same polarization; in periodically poled $LiNbO_3$ (PPLN), a nonlinear material that is used to double the 1064-nm output of Nd:YAG lasers, the resultant nonlinear conversion efficiency is improved 20-fold.

Quasi-phase-matched materials have been used for efficient SHG[12] and optical parametric oscillators.[13] They have also been used to generate squeezed states from optical parametric amplification[14] and from traveling-wave SHG.[15] To date, however, these materials have not been used in a singly resonant doubler to generate bright squeezed light.

2. RESONANT SECOND-HARMONIC GENERATION SQUEEZING THEORY

A derivation of the squeezing spectrum from a singly resonant doubler was previously published.[2] We rederive the results here for the sake of completeness, using lowercase letters to represent operators of cavity modes and uppercase letters to represent operators of photon fluxes entering and leaving the cavity.

The Hamiltonian for the SHG that takes place in the nonlinear material is given by

$$H = i\hbar \frac{\kappa}{2}(a^{\dagger 2} a_{\mathrm{sh}} - a^2 a_{\mathrm{sh}}^{\dagger}), \tag{1}$$

where a is the fundamental cavity mode operator, a_{sh} is the second-harmonic cavity mode operator, and κ is the nonlinear coupling. Commutation with this Hamiltonian gives the equations of motion for the mode operators:

 © 2002 Optical Society of America

$$\dot{a} = -\gamma a + \kappa a^{\dagger} a_{\mathrm{sh}} + \sqrt{2\gamma_0}\, A_{\mathrm{in}} + \sqrt{2\gamma_{\mathrm{loss}}}\, A_{\mathrm{loss}}, \quad (2)$$

$$\dot{a}_{\mathrm{sh}} = -\gamma_{\mathrm{sh}} a_{\mathrm{sh}} - \frac{\kappa}{2} a^2 + \sqrt{2\gamma_{\mathrm{sh}}}\, A_{\mathrm{sh,in}}, \quad (3)$$

where cavity effects have been included through γ, the overall cavity photon loss rate at the fundamental wavelength; γ_0, the photon loss rate through the input coupler with associated input A_{in}; and γ_{loss}, the other photon loss rates at the fundamental wavelength with associated input A_{loss}. The second-harmonic photon loss rates, γ_{sh}, are assumed to be dominated by one mirror with high transmission and associated input $A_{\mathrm{sh,in}}$.

As the second-harmonic wavelength does not resonate within the cavity, its dynamics are much faster than those of the fundamental wavelength. As a result, its mode operator can be treated as a steady-state quantity, giving a single equation of motion for the fundamental mode operator:

$$\dot{a} = -\gamma a - \mu a^{\dagger} a^2 + 2\sqrt{\mu} a^{\dagger} A_{\mathrm{sh,in}} + \sqrt{2\gamma_0}\, A_{\mathrm{in}} + \sqrt{2\gamma_{\mathrm{loss}}}\, A_{\mathrm{loss}}, \quad (4)$$

where $\mu = \kappa^2/2\gamma_{\mathrm{sh}}$ is the two-photon damping rate.

To determine the behavior of small fluctuations within the cavity we express the mode operators in the form $a = \alpha + \delta a$ and $A = A + \delta A$. For the fundamental cavity mode operator, α is the semiclassical steady state given by the steady-state solution to Eq. (4) assuming no steady-state input at the second harmonic:

$$\alpha = \frac{\sqrt{2\gamma_0} A_{\mathrm{in}}}{\gamma + \mu|\alpha|^2}. \quad (5)$$

Without loss of generality, both α and A_{in} may be taken to be real.

The rate equation for the intracavity fluctuations at the fundamental wavelength becomes

$$\dot{\delta}_a = -\gamma \delta a - 2\mu|\alpha|^2 \delta a - \mu \alpha^2 \delta a^{\dagger} + 2\sqrt{\mu}\alpha^* \delta A_{\mathrm{sh,in}} + \sqrt{2\gamma_0}\,\delta A_{\mathrm{in}} + \sqrt{2\gamma_{\mathrm{loss}}}\,\delta A_{\mathrm{loss}}, \quad (6)$$

where we have again assumed that there is no steady-state input at the second harmonic. The equation of motion for fluctuations in the amplitude quadrature-phase operator, $X = a + a^{\dagger}$, is then given by

$$\delta\dot{X} = -(\gamma + 3\mu|\alpha|^2)\delta X + 2\sqrt{\mu}\alpha^* \delta X_{\mathrm{sh,in}} + \sqrt{2\gamma_0}\,\delta X_{\mathrm{in}} + \sqrt{2\gamma_{\mathrm{loss}}}\,\delta X_{\mathrm{loss}}, \quad (7)$$

where $\delta X_i = \delta A_i + \delta A_i^{\dagger}$ for each of the field modes.

To obtain a spectrum of the noise we convert to frequency space by means of a Fourier transform:

$$-i2\pi\Omega\,\delta\tilde{X}(\Omega) = -(\gamma + 3\mu|\alpha|^2)\delta\tilde{X}(\Omega) + 2\sqrt{\mu}\alpha^* \delta\tilde{X}_{\mathrm{sh,in}}(\Omega) + \sqrt{2\gamma_0}\,\delta\tilde{X}_{\mathrm{in}}(\Omega) + \sqrt{2\gamma_{\mathrm{loss}}}\,\delta\tilde{X}_{\mathrm{loss}}(\Omega), \quad (8)$$

where Ω is the frequency in hertz. This expression can be rewritten as

$$\delta\tilde{X}(\Omega) = \frac{\sqrt{2\gamma_0}\,\delta\tilde{X}_{\mathrm{in}}(\Omega) + 2\sqrt{\mu|\alpha|^2}\,\delta\tilde{X}_{\mathrm{sh,in}}(\Omega) + \sqrt{2\gamma_{\mathrm{loss}}}\,\delta\tilde{X}_{\mathrm{loss}}(\Omega)}{\gamma + 3\mu|\alpha|^2 - i2\pi\Omega}. \quad (9)$$

To determine the fluctuations in the quadrature amplitude of the second-harmonic beam leaving the cavity we make use of the boundary condition

$$A_{\mathrm{sh,out}} = \sqrt{\mu} a^2 - A_{\mathrm{sh,in}}, \quad (10)$$

which, in terms of fluctuations, becomes

$$\delta A_{\mathrm{sh,out}} = 2\sqrt{\mu|\alpha|^2}\,\delta a - \delta A_{\mathrm{sh,in}}. \quad (11)$$

So the fluctuations in the second harmonic field exiting the cavity are

$$\delta\tilde{X}_{\mathrm{sh,out}}(\Omega) = 2\sqrt{\mu|\alpha|^2}\,\delta\tilde{X}(\Omega) - \delta\tilde{X}_{\mathrm{sh,in}}(\Omega) = \frac{(-\gamma + \mu|\alpha|^2 + i2\pi\Omega)\,\delta\tilde{X}_{\mathrm{sh,in}}(\Omega) + 2\sqrt{\mu|\alpha|^2}[\sqrt{2\gamma_0}\,\delta\tilde{X}_{\mathrm{in}}(\Omega) + \sqrt{2\gamma_{\mathrm{loss}}}\,\delta\tilde{X}_{\mathrm{loss}}(\Omega)]}{\gamma + 3\mu|\alpha|^2 - i2\pi\Omega}, \quad (12)$$

and the resultant spectrum of the second-harmonic field is

$$V_{\mathrm{sh,out}} = \frac{[(\gamma - \mu|\alpha|^2)^2 + (2\pi\Omega)^2]V_{\mathrm{sh,in}} + 4\mu|\alpha|^2(2\gamma_0 V_{\mathrm{in}} + 2\gamma_{\mathrm{loss}} V_{\mathrm{loss}})}{(\gamma + 3\mu|\alpha|^2)^2 + (2\pi\Omega)^2}, \quad (13)$$

where V is the variance of the fluctuations of the amplitude quadrature-phase operator. If the second-harmonic input and leakage at the fundamental are minimum-uncertainty states, then $V_{\mathrm{sh,in}} = V_{\mathrm{loss}} = 1$, and the resultant spectrum is

$$V_{\mathrm{sh,out}} = 1 + \frac{8\mu|\alpha|^2\{\gamma_0[V_{\mathrm{in}}(\Omega) - 1] - \mu|\alpha|^2\}}{(\gamma + 3\mu|\alpha|^2)^2 + (2\pi\Omega)^2}. \quad (14)$$

This expression for the spectrum of the second-harmonic beam allows the noise characteristics of the pump source, $V_{\mathrm{in}}(\Omega)$, to be included. For the specific

case when the input noise spectrum is that of a minimum-uncertainty state, $V_{\mathrm{in}}(\Omega) = 1$ and the spectrum reduces to

$$V_{\mathrm{sh,out}} = 1 - \frac{8\mu^2|\alpha|^4}{(\gamma + 3\mu|\alpha|^2)^2 + (2\pi\Omega)^2}, \quad (15)$$

which is Eq. (16) of Ref. 2. This expression shows that the maximum amount of squeezing obtainable from ideal singly resonant SHG is $V_{\mathrm{sh,out}} = 1/9$, or 9.5 dB.

3. RELATING THEORY TO EXPERIMENT

To be able to compare the squeezing performance of various cavity configurations and nonlinear materials we need to relate the parameters in the theoretical result to material and cavity parameters. In particular, we need to determine the two-photon damping rate μ, the semiclassical steady-state solution for the intracavity mode operator α, and the cavity photon loss rate γ in terms of measurable quantities.

As was pointed out in Ref. 2, the two-photon damping rate can be related to the conversion efficiency. The power of the second-harmonic field leaving the cavity is given by

$$P_{\mathrm{sh}} = \hbar\omega_2|A_{\mathrm{sh,out}}|^2, \quad (16)$$

where ω_2 is the optical frequency of the second-harmonic beam. Using boundary condition Eq. (10) for the semiclassical solution, we can rewrite Eq. (16) as

$$P_{\mathrm{sh}} = 2\hbar\omega_1\mu|\alpha|^4, \quad (17)$$

where ω_1 is the optical frequency of the fundamental beam and α is related to the circulating pump power by

$$|\alpha|^2 = \frac{\tau P_{\mathrm{circ}}}{\hbar\omega_1}. \quad (18)$$

Thus the second-harmonic power exiting the cavity is related to the circulating pump power by

$$\frac{P_{\mathrm{sh}}}{P_{\mathrm{circ}}} = \frac{2\mu\tau^2}{\hbar\omega_1}P_{\mathrm{circ}} = \gamma_{\mathrm{sh}}P_{\mathrm{circ}}, \quad (19)$$

which is equivalent to Eq. (7) of Ref. 2.

For a Gaussian beam passing through a nonlinear material the conversion efficiency is given by[16]

$$\gamma_{\mathrm{sh}} = \frac{d_{\mathrm{eff}}^2 h 16\pi^2 l}{\lambda^3 n_{\omega_1} n_{\omega_2}\epsilon_0 c}, \quad (20)$$

where d_{eff} is the effective nonlinear coefficient of the nonlinear material, h is the Boyd–Kleinman focusing factor, l is the crystal length, λ is the fundamental wavelength, n_ω is the index of refraction of the nonlinear material at optical frequency ω, ϵ_0 is the permittivity of free space, and c is the speed of light.

As a result, the two-photon damping rate, μ, can be expressed in terms of material and cavity parameters:

$$\mu = \frac{\hbar\omega_1}{2\tau^2}\frac{d_{\mathrm{eff}}^2 h 16\pi^2 l}{\lambda^3 n_{\omega_1} n_{\omega_2}\epsilon_0 c}. \quad (21)$$

Finally, using the relationship

$$|A_{\mathrm{in}}|^2 = P_{\mathrm{in}}/\hbar\omega_1 \quad (22)$$

together with Eq. (5), we can numerically determine α for a given incident power.

The cavity photon loss rate is all that remains to be determined to enable us to calculate the spectrum of the second-harmonic output.

4. CAVITY DESIGN AND NONLINEARITY

Four cavity designs for a singly resonant doubler are shown in Fig. 1. All cavities are defined by an input coupler with power reflectivity R_1 at the fundamental wavelength and an end mirror with power reflectivity R_2. One of these two mirrors will be highly transmissive at the second harmonic (shown as mirror 2 here) and the other highly reflective. The nonlinear crystal is of length l, with incident power P_{in}, circulating power P_{circ}, and output second-harmonic power P_{sh}.

The free-space cavity shown in Fig. 1a consists of a crystal placed between two mirrors. For this configuration the photon loss rate is given by

$$\gamma = \gamma_0 + \gamma_{\mathrm{loss}} = {}^1/_2\mathrm{FSR}[2 - R_1 - (1 - \delta_c)^4(1 - \delta_a)^2 R_2], \quad (23)$$

where FSR is the cavity free spectral range given by $c/2[L + (n_\omega - 1)l]$, L is the overall cavity length, δ_c is the loss in the crystal coating, and δ_a is the loss that is due to absorption within the crystal. The conversion efficiency for this cavity design is four times that in Eq. (20). The extra factor of 4 arises because the focused fundamental wavelength beam passes twice through the crystal in a cavity round trip, provided that the correct phase is maintained between the fundamental beam and the second-harmonic beam and, if required, the periodic domains in the nonlinear material.[17]

In the hemilithic cavity, Fig. 1b, one face of the crystal is used as one of the cavity mirrors. In this configuration the conversion efficiency remains the same as for the free-space cavity (if the crystal length and beam focusing remain the same), but the cavity photon loss rate becomes

$$\gamma = {}^1/_2\mathrm{FSR}[2 - R_1 - (1 - \delta_c)^2(1 - \delta_a)^2 R_2]. \quad (24)$$

It is reduced because the crystal coating interface is passed only twice within a cavity round trip.

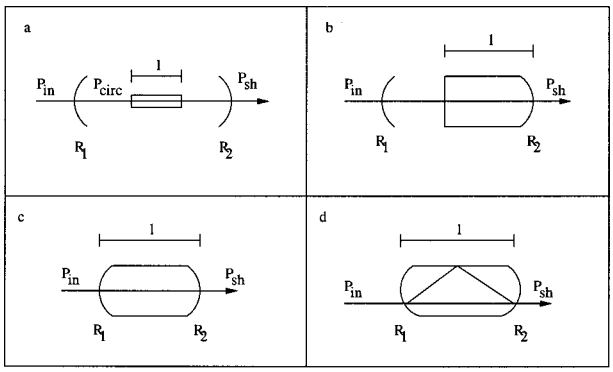

Fig. 1. Possible single-resonator configurations: a, free-space; b, hemilithic; c, monolithic; d, ring monolithic.

In the linear monolithic cavity, Fig. 1c, the cavity is defined by both faces of the crystal. In this case the cavity loss is reduced further to

$$\gamma = {}^1/_2\mathrm{FSR}[2 - R_1 - (1 - \delta_a)^2 R_2], \tag{25}$$

and the cavity free spectral range is now simply $c/2n_\omega l$.

For poled materials, some care must be taken when one is attempting a monolithic design. After one trip through the crystal, both fundamental and second-harmonic beams are present. These two beams must be in phase with each other as well as with the alternating poled regions within the crystal on the return trip. If they are not, backconversion will occur and the overall nonlinearity will be reduced. Several techniques, such as tilting the birefingent crystal and controlling the phase-matching temperature, can be used to solve this phase problem, but several factors have prevented their widespread use.[17]

A ring monolithic resonator, as shown in Fig. 1d, offers some experimental advantages. First, conversion occurs only during the horizontal part of the round trip. During the diagonal paths there is no phase matching, so no conversion occurs. By the time that the fundamental beam completes a round trip, the second-harmonic beam has left the cavity, so no backconversion can occur. Additionally, removing the second harmonic after a round trip will help to prevent competing nonlinear interactions, which have been shown to limit squeezing and may introduce undesirable dynamic effects.[18] However, in a ring monolithic resonator the conversion, γ_{sh}, is reduced by a factor of 4 from that for the other designs and is equal to that in Eq. (20).

We can now predict the performance of each of these configurations for either poled or unpoled lithium niobate.

5. COMPARISON OF PERFORMANCE

The theoretical conversion efficiencies for the various cavity geometries are shown in Fig. 2. For all cavities the crystal length is assumed to be 1 cm, with 0.1-m^{-1} absorption and a coating transmission of 99.4%. The input coupling is $R_1 = 99\%$, and end mirrors have reflectivity $R_2 = 99.9\%$ at the fundamental wavelength. All cavities are assumed to have a Boyd–Kleinman focusing factor $h = 0.7$. The free-space cavity is 5 cm long, and the hemilithic cavity is 2.5 cm long. The results for birefringently phase-matched lithium niobate are shown by dashed curves, and those for periodically poled crystals are shown by solid curves. The PPLN monolithic cavity is assumed to be the ring geometry with modified conversion, as explained above.

As expected, the lower-loss cavities reach the maximum in their efficiencies at lower input powers. From Eqs. (5), (17), and (22),

$$\frac{P_{\mathrm{sh}}}{P_{\mathrm{in}}} = \frac{4\mu\gamma_0|\alpha|^2}{(\gamma + \mu|\alpha|^2)^2}, \tag{26}$$

which reaches the maximum of

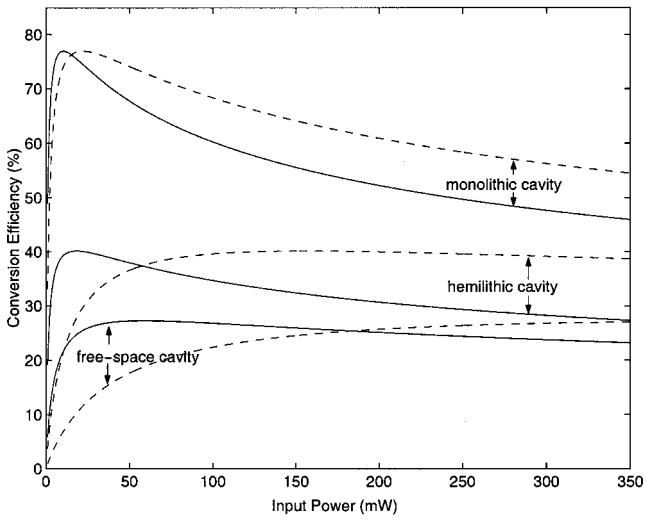

Fig. 2. Conversion efficiencies for several cavity configurations with $LiNbO_3$ nonlinear crystals. Dashed curves, birefringently phase matched; solid curves, quasi-phase matched. Parameter values are $L = 1$ cm, $R_1 = 99\%$, $R_2 = 99.9\%$, $\delta_c = 0.6\%$, $\delta_a = 0.1\%$, and $h = 0.7$. The free-space cavity is 5 cm long, and the hemilithic cavity is 2.5 cm long.

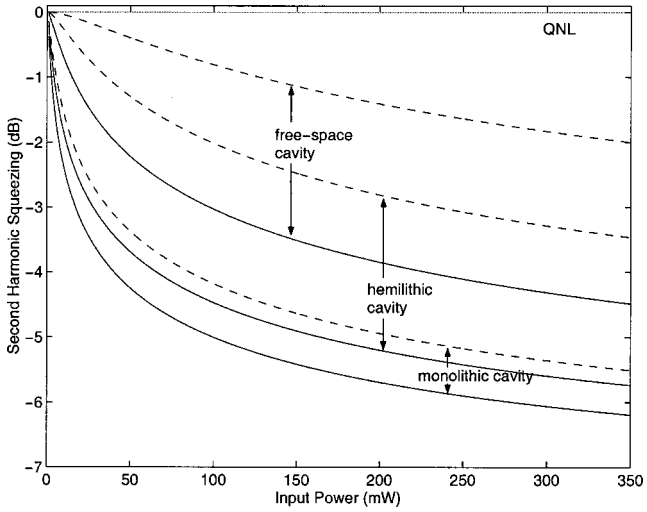

Fig. 3. Squeezed output at 12 MHz for several cavity configurations, with cavity parameter values as in Fig. 2. The results for birefringently phase-matched $LiNbO_3$ are shown by dashed curves, and those for periodically poled crystals are shown by solid curves. QNL, quantum-noise limit.

$$\frac{P_{\mathrm{sh}}}{P_{\mathrm{in}}} = \frac{\gamma_0}{\gamma} \tag{27}$$

when $\gamma = \mu|\alpha|^2$.

For lower losses γ, this condition is met at a lower value of α, and hence at a lower input power, for a fixed nonlinearity μ. Similarly, the maximum efficiency occurs at a lower input power for cavities with periodically poled crystals. Here the higher nonlinearity at an equal loss means that the maximum conversion condition is met at a lower input power.

Squeezing of the second-harmonic output at 12 MHz is shown in Fig. 3 for the three cavities. At this frequency it is assumed that the input laser noise has been reduced

to the standard quantum limit by means of a ring-mode cleaner. These results clearly show the advantage of lower-loss cavities and higher nonlinearity materials, even for the ring monolithic case with reduced nonlinearity. It should also be noted that the parameters used for these results (the same values as used for the efficiency curves) have not been chosen to maximize the squeezing but rather are values easily attainable experimentally.

As well, note that the squeezing increases past the point of maximum conversion. At maximum conversion, the squeezing spectrum, Eq. (15) becomes

$$V_{\mathrm{sh,out}} = 1 - \frac{8\mu^2|\alpha|^4}{16\mu^2|\alpha|^4 + (2\pi\Omega)^2} \approx 1/2 \qquad (28)$$

for sufficiently low frequencies ($2\pi\Omega \ll 4\mu|\alpha|^2$). Hence the squeezing in the second-harmonic beam will be ~3 dB at the point of maximum conversion efficiency and should increase beyond that point. For those cavities that pass through the maximum conversion efficiency, we see that such is indeed the case.

There are experimental trade-offs that exist when one is selecting the cavities. The free-space cavity requires only simple crystal fabrication and can be quickly and easily altered with different mirrors to adapt its input power impedance matching point[6] to available laser sources. However, obtaining squeezing at a relatively low frequency requires that the photon loss rate be kept as small as possible, which can be experimentally challenging, as the cavity must contain both a crystal and an oven.

The hemilithic cavity requires the fabrication of a curved end face on the crystal but is more easily incorporated into a small cavity. As well, only one cavity mirror is separate from the crystal, so the cavity is less sensitive to any mechanical vibrations than the free-space cavity.

Whereas the monolithic cavity provides the least amount of loss and the greatest amount of mechanical stability, it comes at the price of requiring a significant amount of crystal fabrication. However, the improved squeezing output makes the monolithic cavity the obvious choice when one is trying to produce optimally squeezed SHG. We had no such sample available, so we proceeded with a free-space cavity for the experimental demonstration.

6. EXPERIMENTAL WORK

The setup for our free-space cavity experiment is shown in Fig. 4. The crystal was a 1-cm long piece of PPLN wedged at one end to permit double-pass SHG, as described in Ref. 17. The laser source was a 1.5-W 1064-nm Nd:YAG nonplanar ring oscillator that was tilt locked[19] to the high-finesse ($F \approx 400$) mode of a ring-mode cleaner similar in design to that described in Ref. 4. The beam was then phase modulated, and the reflection from the doubling cavity was used to lock the cavity by the Pound–Drever–Hall technique.[20] The green output was separated from the infrared by means of a dichroic beam splitter and then sent to a 50/50 beam splitter. The resultant beams were sent to two balanced detectors whose currents were either added or subtracted and measured on a spectrum analyzer.

The spectrum analyzer was swept over a range of a few megahertz, centered at 11.5 MHz, for each input power. During a single run the signal sent to the spectrum analyzer was toggled between the sum and the difference of the currents from the detectors. A sample of our data is shown in Fig. 5. The higher segments of the data are from the difference of the currents, the quantum-noise limit. The lower segments are from the sum of the currents and show the squeezing on our beam.[1] The sharp downward spikes between segments are transients that are due to the toggling action between the two signals. The overall downward trend is due to the frequency response of the balanced detectors.

We converted the raw data into squeezed output by taking the difference between the two extremes, and the results are shown in Fig. 6 along with the theoretical pre-

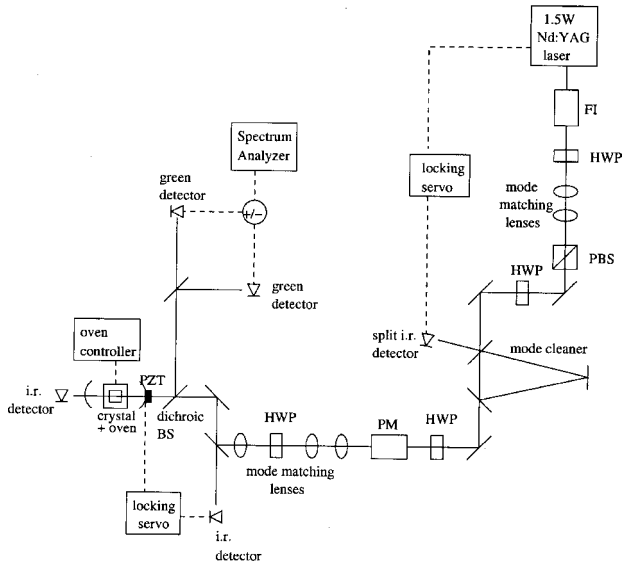

Fig. 4. Experimental setup with a PPLN free-space cavity. The single-axial-mode Nd:YAG laser is passed through a Faraday isolator (FI), followed by a half-wave plate (HWP) and a polarizing beam splitter (PBS) to adjust the power incident upon the SHG cavity. This laser was locked to a mode cleaner by means of tilt locking.[19] The phase modulator (PM) is required for the Pound–Drever–Hall locking of the free-space cavity.[20] The length of the free-space cavity is controlled by a piezo-actuated mirror (PZT).

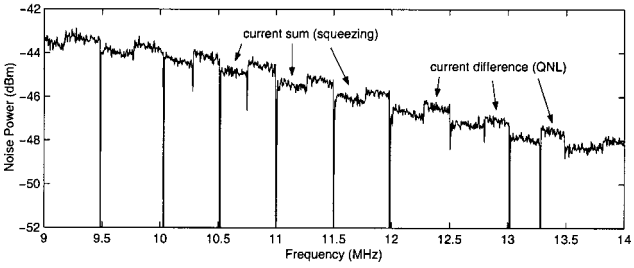

Fig. 5. Raw data from a PPLN free-space cavity. The higher segments show the quantum-noise limit. The lower segments show the squeezing on our beam. The sharp downward spikes between segments are transients that are due to toggling between the two signals. The overall downward trend is due to frequency responses of the balanced detectors. QNL, quantum-noise limit.

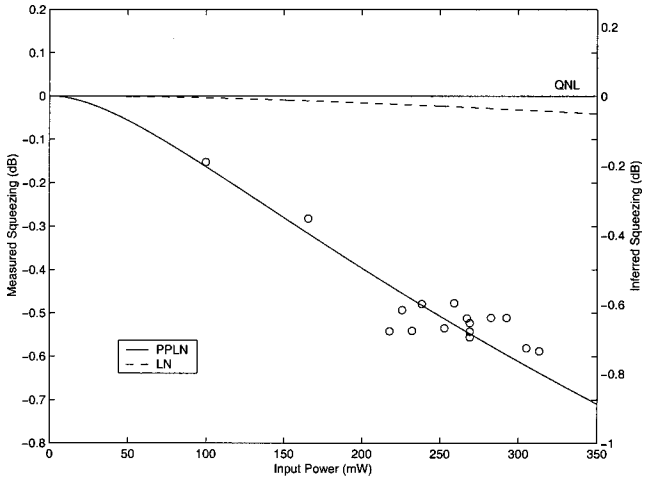

Fig. 6. PPLN free-space cavity experimental results (open circles) and theoretical fit (solid curves). The cavity photon loss rate was the fitted parameter with a value of 180 MHz. The other cavity parameters are as in Fig. 3. The dashed curve indicates the theoretical performance of an identical cavity with birefringently phase-matched $LiNbO_3$.

dictions for our experiment. The only free parameter in our theoretical fit was the cavity photon loss rate, γ. The fitted value, 180 MHz, is higher than expected, probably because of clipping of the beam within the cavity. This is one of the risks of using a free-space cavity for which the crystal and the oven must be placed within the cavity mirrors. The other experimental parameters are the same as those used for the theoretical modeling of the free-space cavity described in Section 5.

The right-hand axis of Fig. 6 indicates the inferred amount of squeezing, taking into account the measured detector quantum efficiencies of 86%. The dashed curve shows the theoretical performance of a theoretical cavity with exactly the same parameter values but with a birefringently phase-matched $LiNbO_3$ sample. As can be seen, the squeezing in the output from such a cavity would be difficult to measure.

7. CONCLUSIONS

We have successfully measured the squeezing from a singly resonant doubler with a crystal of periodically poled lithium niobate as the nonlinear medium. Our experiment behaved as predicted by theory, yielding slightly less than 0.6 dB of directly measured squeezing or greater than 0.7 dB of inferred squeezing. Under slightly better operating conditions, our output was measured to have 1 dB of squeezing, but unfortunately this amount of squeezing was not reproducible for a variety of experimental reasons, particularly the mechanical instability of our cavity and increased losses.

From the application of theory to the possible cavity designs, the monolithic PPLN cavity is a promising source of bright squeezed light. Further optimization from the theoretical results shown here may be possible, with such improvements as longer cavities and better coatings. A singly resonant doubler with more than 6 dB of squeezing at moderate input power levels should be possible.

ACKNOWLEDGMENTS

M. J. Lawrence acknowledges the hospitality of the Department of Physics, Australian National University, where the experimental work was performed.

REFERENCES

1. S. F. Pereira, M. Xiao, H. J. Kimble, and J. L. Hall, "Generation of squeezed light by intracavity frequency doubling," Phys. Rev. A **38**, 4931–4934 (1988).
2. R. Paschotta, M. Collett, P. Kürz, K. Fiedler, H.-A. Bachor, and J. Mlynek, "Bright squeezed light from a singly resonant frequency doubler," Phys. Rev. Lett. **72**, 3807–3810 (1994).
3. T. C. Ralph, M. S. Taubman, A. G. White, D. E. McClelland, and H.-A. Bachor, "Squeezed light from second-harmonic generation: experiment versus theory," Opt. Lett. **20**, 1316–1318 (1995).
4. B. Willke, N. Uehara, E. K. Gustafson, R. L. Byer, P. J. King, S. U. Seel, and R. L. Savage, Jr., "Spatial and temporal filtering of a 10-W Nd:YAG laser with a Fabry–Perot ring-cavity premode cleaner," Opt. Lett. **23**, 1704–1706 (1998).
5. A. G. White, M. S. Taubman, T. C. Ralph, P. K. Lam, D. E. McClelland, and H.-A. Bachor, "Experimental test of modular noise propagation theory for quantum optics," Phys. Rev. A **54**, 3400–3404 (1996).
6. W. J. Kozlovsky, C. D. Nabors, and R. L. Byer, "Efficient second-harmonic generation of a diode-laser-pumped cw Nd:YAG laser using monolithic MgO:$LiNbO_3$ external resonant cavities," IEEE J. Quantum Electron. **24**, 913–919 (1988).
7. S. Schiller and R. L. Byer, "Quadruply resonant optical parametric oscillation in a monolithic total-internal-reflection resonator," J. Opt. Soc. Am. B **10**, 1696–1707 (1993).
8. P. Kürz, R. Paschotta, K. Fiedler, and J. Mlynek, "Squeezing by second-harmonic generation in a monolithic resonator," Appl. Phys. B **55**, 216–225 (1992).
9. G. Breitenbach, T. Müller, S. F. Pereira, J.-Ph. Poizat, S. Schiller, and J. Mlynek, "Squeezed vacuum from a monolithic optical parametric oscillator," J. Opt. Soc. Am. B **12**, 2304–2309 (1995).
10. P. K. Lam, T. C. Ralph, B. C. Buchler, D. E. McClelland, H.-A. Bachor, and J. Gao, "Optimization and transfer of vacuum squeezing from an optical parametric oscillator," J. Opt. B **1**, 469–474 (1999).
11. M. M. Fejer, G. A. Magel, D. H. Jundt, and R. L. Byer, "Quasi-phase-matched second harmonic generation: tuning and tolerances," IEEE J. Quantum Electron. **28**, 2631–2654 (1992).
12. G. D. Miller, R. G. Batchko, W. M. Tulloch, D. R. Weise, M. M. Fejer, and R. L. Byer, "42% efficient single-pass cw second harmonic generation in periodically poled lithium niobate," Opt. Lett. **22**, 1834–1836 (1997).
13. L. E. Myers, G. D. Miller, R. C. Eckardt, M. M. Fejer, R. L. Byer, and W. R. Bosenberg, "Quasi-phase-matched optical parametric oscillator in bulk periodically poled $LiNbO_3$," Opt. Lett. **20**, 52–54 (1995).
14. D. K. Serkland, M. M. Fejer, R. L. Byer, and Y. Yamamoto, "Squeezing in a quasi-phase-matched $LiNbO_3$ waveguide," Opt. Lett. **20**, 1649–1652 (1995).
15. D. K. Serkland, P. Kumar, M. A. Arbore, and M. M. Fejer, "Amplitude squeezing by means of quasi-phase-matched second-harmonic generation in a lithium niobate waveguide," Opt. Lett. **22**, 1497–1499 (1997).
16. G. D. Boyd and D. A. Kleinman, "Parametric interaction of focused Gaussian light beams," J. Appl. Phys. **39**, 3597–3639 (1968).
17. G. Imeshev, M. Proctor, and M. M. Fejer, "Phase correction in double-pass quasi-phase-matched second-harmonic generation with a wedged crystal," Opt. Lett. **23**, 165–167 (1998).

18. A. G. White, P. K. Lam, M. S. Taubman, M. A. M. Marte, S. Schiller, D. E. McClelland, and H.-A. Bachor, "Classical and quantum signatures of competing $\chi^{(2)}$ nonlinearities," Phys. Rev. A **55**, 4511–4515 (1997).
19. D. A. Shaddock, M. B. Gray, and D. E. McClelland, "Frequency locking a laser to an optical cavity by use of spatial mode interference," Opt. Lett. **24**, 1499–1501 (1999).
20. R. W. P. Drever, J. L. Hall, F. W. Kowalski, J. Hough, G. M. Ford, A. J. Munley, and H. Ward, "Laser phase and frequency stabilization using an optical resonator," Appl. Phys. B **31**, 97–105 (1983).